New Frontier in Hypericin-Mediated Diagnosis of Cancer with Current Optical Technologies

Malini Olivo,[1,2,3,4] Chit Yaw Fu,[1] Vijaya Raghavan,[1] and Weber Kam On Lau[5]

[1]School of Physics, National University of Ireland, Galway, Ireland; [2]Bio-optical Imaging Group, Singapore Bioimaging Consortium, Agency for Science, Technology and Research, Singapore, Singapore; [3]Department of Pharmacy, National University of Singapore, Singapore, Singapore; [4]National Cancer Centre Singapore, Singapore, Singapore; and [5]Department of Urology, Singapore General Hospital, Singapore, Singapore

Associate Editor Daniel Elson oversaw the review of this article.

Abstract—Photosensitizers (PSs) have shown great potentials as molecular contrast agents in photodynamic diagnosis (PDD) of cancer. While the diagnostic values of PSs have been proven previously, little efforts have been put into developing optical imaging and diagnostic algorithms. In this article, we review the recent development of optical probes that have been used in conjunction with a potent PS, hypericin (HY). Various fluorescence techniques such as laser confocal microscopy, fluorescence urine cytology, endoscopy and endomicroscopy are covered. We will also discuss about image processing and classification approaches employed for accurate PDD. We anticipate that continual efforts in these developments could lead to an objective PDD and complete surgical clearance of tumors. Recent advancements in nanotechnology have also opened new horizons for PSs. The use of biocompatible gold nanoparticles as carrier for enhanced targeted delivery of HY has been attained. In addition, plasmonic properties of nanoparticles were harnessed to induce localized hyperthermia and to manage the release of PS molecules, enabling a better therapeutic outcome of a combined photodynamic and photothermal therapy. Finally, we discuss how nanoparticles can be used as contrast agents for other optical techniques such as optical coherence tomography and surface-enhanced Raman scattering imaging.

Keywords—Hypericin, Photodynamic diagnosis, Fluorescence, Endoscopy, Urine cytology, Endomicroscopy, Gold nanoparticle, Photothermal therapy.

INTRODUCTION

Successful detection of cancer onset and surgical clearance of tumor certainly help to increase the rate of survival without recurrence.[60,62] Current diagnosis and surgical procedures depend largely on visual inspection using a primitive white-light endoscope (WLE). However, the given diagnostic information about the tissue has always been inadequate for an objective assessment that has a decisive impact on the therapeutic outcome. Many optical techniques[82,94,101,103] are capable of acquiring rich diagnostic information and signaling any subtle changes occurring in tissue optics and biochemistry. These imaging techniques, therefore, provide a means of visualizing the structural and molecular contrast between healthy and cancerous tissues. This visual aid can potentially be a useful adjunct to complete resection of multifocal tumors.

While these optical diagnostic techniques are typically used in research laboratories, some of which are being translated to clinical practice.[4,28,59,88] Advancements in fiber optics, optoelectronics, and microactuators have provided cost-effective solutions to the integration of these optical diagnostics into an existing catheter or endoscope that is being used as a navigation aid in standard diagnosis. Regardless of the techniques used, the measured optical signals are essentially correlated with the pathological status of the tissues that can vary the light-tissue interactions by light absorption, scattering, and emission. The acquired data, in general, is overwhelming, and thus needs to be modeled and condensed into a set of concise diagnostic parameters from which a diagnostic algorithm can be derived to perform a light-guided biopsy and surgery.

Photosensitizers (PSs) are light-triggered drugs specially used in photodynamic therapy (PDT) to eradicate cancerous cells.[16] PSs are also fluorescent compounds with preferential uptake by tumors. These

---

Address correspondence to Malini Olivo, School of Physics, National University of Ireland, Galway, Ireland. Electronic mail: malini.olivo@nuigalway.ie

attributes make PS a promising biomarker to diagnose cancer using fluorescence techniques. Such optical diagnoses are now commonly referred to as photodynamic diagnosis (PDD). PDD of cancer has found its way into widespread clinical use, and the diagnostic values of PDD agents have already been reviewed.[33,34,44] While the photosensitizing and chemical properties of PSs have been much studied,[37] less emphasis is given to the probe design and diagnostic algorithms that also have an impact on the diagnostic accuracy. A fair evaluation of these aspects among different groups is usually difficult because the diagnostic outcomes depend on several factors including cancer types, PS administration, and formulation. In this review article, we narrow our focus to discussion on PDD using hypericin (HY), a potent PS, which our group has been investigating with customized instruments and diagnostic algorithms developed to aid quantitative and objective analysis. In addition to the diagnostic values from HY fluorescence, our group also attempts to couple HY with nanoparticles to extend its use in other optical imaging techniques.

This review is divided up as follows: First, PDD of cancer using PSs is discussed and compared with autofluorescence diagnosis. Second, the fluorescence properties of HY and issues surrounding its solubility and targeted delivery are presented. Third, studies of HY-PDD used with assorted fluorescence diagnostic devices are detailed; this section highlights the recent development of optical instruments and diagnostic algorithms for directing biopsies and assessing resection margins for lesions. While HY is widely used in PDD and PDT, its use can be further extended to other regimes. The following section summarizes the underlying trend in nanotechnology that gradually reinforces the use of HY for combined therapeutics and multimodality imaging.

FLUORESCENCE DIAGNOSIS OF CANCER

Fluorescence diagnosis of cancer utilizes the characteristic fluorescence signatures, either from inherent or exogenous fluorophores, to distinguish abnormal tissues from surrounding normal tissues. If the fluorescence signatures of inherent biomolecules are utilized, then the diagnostic technique is termed as Autofluorescence diagnosis, and Exogenous fluorescence diagnosis, if exogenous fluorophores are used.

Autofluorescence Diagnosis

Successful autofluorescence diagnosis has been previously reported to distinguish normal from malignant tissues. For instance, Koenig *et al.*[49] conducted cancer diagnosis by comparing the autofluorescence spectra of the tissues excited at 337 nm. By calculating the fluorescence intensity ratios at 385 and 455 nm, the autofluorescence signal from collagen and reduced nicotinamide adenine dinucleotide (NADH), respectively, the study could discern normal and malignant lesions with sensitivity and specificity of 97 and 98%, respectively. Another autofluorescence study by Zaak *et al.*,[108]—using different intensity ratios at 335 and 430 nm, corresponding to signals from tryptophan-rich proteins and NADH, respectively—distinguished malignant from benign lesions with sensitivity and specificity of 95 and 77%, respectively. Similarly, fluorescence endoscopy has also been utilized in discerning normal from cancerous lesions, where the extent of loss in autofluorescence emission in the green region of the visible spectrum was considered the distinguishing parameter.[51,70]

However, most of these endogenous fluorophores weakly fluoresce even when excited optimally at UV-blue region (300–450 nm). In addition, the penetration depth of UV-blue light in tissue is often limited by high tissue scattering and strong absorption of hemoglobin in 400–500 nm region.[69] The epithelial thickening, which typically occurs in tumors, can further reduce the amount of excitation light reaching the inner submucosa where most endogenous fluorophores are located. The failure in probing the fluorescence emission from deeper layers presented limitation in distinguishing carcinoma from dysplasia and carcinoma *in situ* (CIS).[11,51]

Exogenous Fluorescence Diagnosis

Exogenous fluorescence diagnosis uses synthetic fluorophores, which are excitable at longer wavelength, to visualize neoplastic lesions that cannot be seen using white-light imaging and autofluorescence imaging. Unlike autofluorescence, exogenous fluorescence diagnosis relies on positive fluorescence staining of malignant and pre-malignant lesions. This reflected in increased detection of dysplasia and CIS, and discerning of these from malignant tumors.[34,102] Currently, the exogenous fluorophores used in clinical environment are PS. PSs are compounds that, along with fluorescing capability, have favorable diagnostic characteristics, such as tumor specificity, rapid pharmacokinetic elimination, low levels of dark-toxicity, *etc.*[6] HY, 5-aminolevulinic acid (ALA) and its derivatives, like 5-ALA hexylester, are prominent among PSs that are being evaluated for its clinical utility. These PSs are traditionally used in PDT for its aforementioned properties, and when used for diagnostic purposes, the technique is termed as PDD. PDD, as an alternative diagnostic technique, has already been

approved for bladder cancer in European Union (EU) and European Economic Area (EEA).[11,109]

Ideal Photodynamic Diagnosis Agent

5-aminolevulinic acid is a PS that induces and accumulates fluorescent protoporphyrin IX (PpIX), and was initially reported by Kennedy *et al.*[45] and Kreigmair *et al.*[34] Though 5-ALA was widely investigated, it faced shortcomings like fast photobleaching of induced PpIX and less tissue penetration due to low lipophilicity and lower specificity. Subsequently, various derivatives of 5-ALA were also investigated with little success. Then D'Hallewin *et al.*[12] identified HY as a better choice of PS used for detecting bladder cancer. Though the diagnosis with 5-ALA (78–100%) has sensitivity comparable to HY (82–94%),[75] it was shown to yield low specificity ranging from 41 to 66%,[34] which implies many false positives. On the other hand, studies that investigated HY for fluorescence diagnosis reported excellent sensitivity along with superior specificity ranging from 91[81] to 98%,[12] which greatly reduces the incidence of false positive results. Later studies continue to report HY's advantages over other drugs, in fluorescence diagnosis and PDT[87] of various cancers.[51,56,64,89,109,111]

PHOTODYNAMIC PROPERTIES OF HYPERICIN

Fluorescence Properties

Hypericin is extracted from a plant, *Hypericum perforatum* L., commonly known as St. John's Wort. HY consistently exhibited well-resolved spectral bands when dissolved in various organic solvents, with absorption maxima at around 540 and 590 nm, and fluorescence maxima at around 590 and 640 nm.[11,97,100] Absorption maxima of HY being at longer wavelength allows excitation light to reach HY in deeper tumors whereas light that excites 5-ALA-induced PpIX with absorption maxima at around 400 nm can only penetrate shallowly into tissue. Another important property of HY making it a prime PS in PDD is its photostability, as reported by various studies, and its fluorescence could be detected for up to 16 h after instillation. Its photostability could be further enhanced when formulated with 40% *N*-methyl pyrrolidone (NMP).[77]

Tumor Selectivity of Hypericin

Despite the fact that HY exhibits tumor selectivity, the specific mechanism involving the cellular uptake is yet to be fully understood. The possible mechanism of preferential HY accumulation in cancerous cells has been reviewed elsewhere.[78] In brief, it has been proposed that both diffusion and endocytosis contribute to the overall transport of HY into individual cancerous cells.[78] Olivo *et al.*[66] showed that HY indeed preferentially localizes in the tumor and the intensity of microscopic HY fluorescence increased with both stage and histological grade of bladder cancer. For instance, the HY intensity of grade 3 cancerous cells was shown to be nearly 3 times higher than of grade 1 cells.

In addition to the fact that intracellular uptake of HY is higher in cancerous cells, subsequent studies unraveled other possible contributing factors to its selective accumulation at tissue level.[30,68] For instance, Huygens *et al.*[30] studied human bladder cell carcinoma using a 3-dimensional (3D) spheroid model, and reported that the loss in intercellular adhesion due to the reduced expression of a transmembrane adhesion protein, E-cadherin, plays a pivotal role in the selective uptake of HY. Later, Olivo *et al.*[68] conducted further studies to evaluate the expression of other cell-adhesion molecules (E-cadherin, α-catenin, β-catenin, and γ-catenin) in histologically graded biopsies obtained after intravesical instillation of HY. In particular, using immunofluorescence staining, E-cadherin expression was found to decrease in proportion to both the tumor grade as well as the depth of invasion. In addition, mRNA analysis showed that expression of E-cadherin and β-catenin was down regulated in high-grade urothelial cell carcinoma (UCC), modifying the histoarchitecture in bladder tumor and decreasing the epithelial paracellular barrier function. This eventually leads to enhanced paracellular diffusion of HY into the deeper layers of tissue before intracellular uptake. Hence, stronger HY fluorescence in the UCC was observed with increased grade and advanced stage. The fluorescence imaging showed that the HY intensity of grade 1, 2, and 3 tissues was approximately 5.4, 8.4, and 10.4 times greater than that of normal bladder tissues.[68]

Solubility and Delivery

Hypericin is a lipophilic compound that forms aggregates and sparingly dissolves in aqueous solution. Different solvents have been tried to overcome this hydrophobicity of HY. These include organic solvents, such as ethanol, tetrahydrofuran, and acetone, and also serum proteins which are reported to dissolve most hydrophobic compounds.[34,74,76,100] Therefore, the focus of recent studies by research groups involved in fluorescence diagnosis of cancer is directed toward new formulations to be used with HY, like using Solketal as absorption enhancer,[42] polyvinylpyrrolidone (PVP)[93] and cyclodextrins as solubilizers,[78] and

NMP as penetration enhancer.[76] For example, our lab investigated HY formulated with different concentrations of NMP and found effective solubilizing and delivery of HY to the target site, bladder urothelium in this study.[77] Subsequently, our *in vitro* study with MGH cell line and *in vivo* studies showed that HY with 0.05% NMP yielded optimal uptake and cell survival. Its delivery efficacy was found to be superior to HY with human serum albumin, which is being clinically used for PDD.[76,101] However, further studies are warranted to determine the optimal concentration of NMP, which solubilizes HY and enhances its tissue penetration without compromising uptake and cell survival.

HYPERICIN-MEDIATED PDD OF CANCER WITH VITAL FLUORESCENCE TECHNOLOGIES

D'Hallewin *et al.*[12] first reported the clinical use of HY-induced PDD in detecting flat CIS lesions of bladder. Thereafter, studies of HY mostly focused on the detection of bladder cancer.[14,43,81] Apart from bladder screening, the applications of HY were also extended to diagnosing other types of cancers including oral cancer[88] and stomach cancer.[15,58] The following sub-sections will mainly discuss about the development of instrumentation and data processing for HY-PDD of bladder and oral cancer.

Microscopic Fluorescence Studies and Diagnosis

Following the pilot study of HY-PDD by D'Hallewin *et al.*,[12] Olivo *et al.*[66] investigated the microscopic fluorescence properties of HY in human bladder cancer.

Spectrofluorometric study of the bladder cancer cell lines revealed rapid uptake of HY as early as 15 min from incubation, and fast clearance from cells within 48 h. Maximum fluorescence intensity was detected between 2 and 3 h, and this determined the optimum intravesical instillation time of HY for screening bladder cancer using a fluorescence endoscope (FE). A clinical evaluation was then carried out with 30 patients comparing FE with conventional WLE. Under blue-light illumination using FE, fluorescence emission of HY was induced, and biopsies were taken from those fluorescent regions for microscopic fluorescence analysis and histopathological grading (see Fig. 1). With the aid of a laser confocal microscopy (LCM), the HY retained in the tissues was optically excited at 488 nm, and a distinct fluorescence distribution across the tissue section was observed from the transitional cell carcinoma (TCC) and CIS lesions. The intensity of the microscopic HY fluorescence increased with both stage (Ta, T1, and T2), and histological grade of bladder cancer (G1–G3), as shown in Fig. 2. In particular, this PDD method enabled an early detection of CIS and other flat lesions, which are frequently overlooked due to poor contrast given by WLE. These microscopic studies evidenced that PDD with HY could be used as a diagnostic aid to conventional histopathology. These microfluorescence properties of HY were later utilized in fluorescence urine cytology.
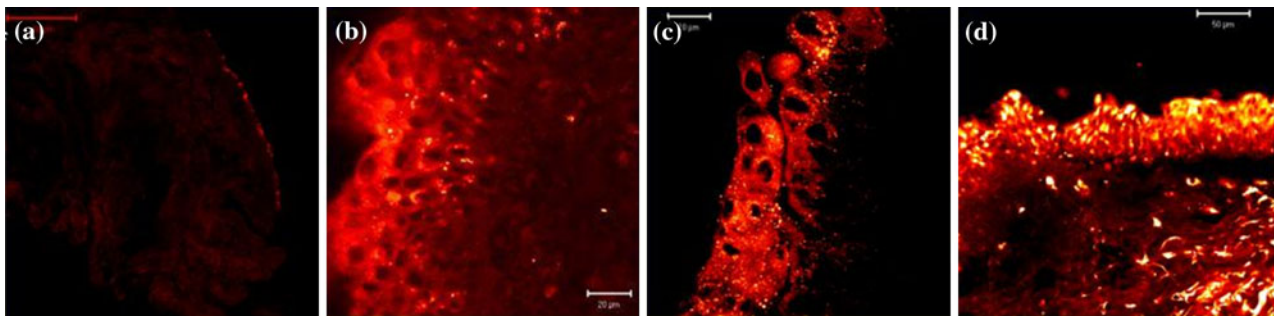
Ex Vivo Urine Cytology

White-light endoscope combined with random biopsy has been the gold standard for a definitive diagnosis of bladder tumors. However, the examination procedure is time-consuming and is associated with patient discomfort. Thus, a non-invasive and
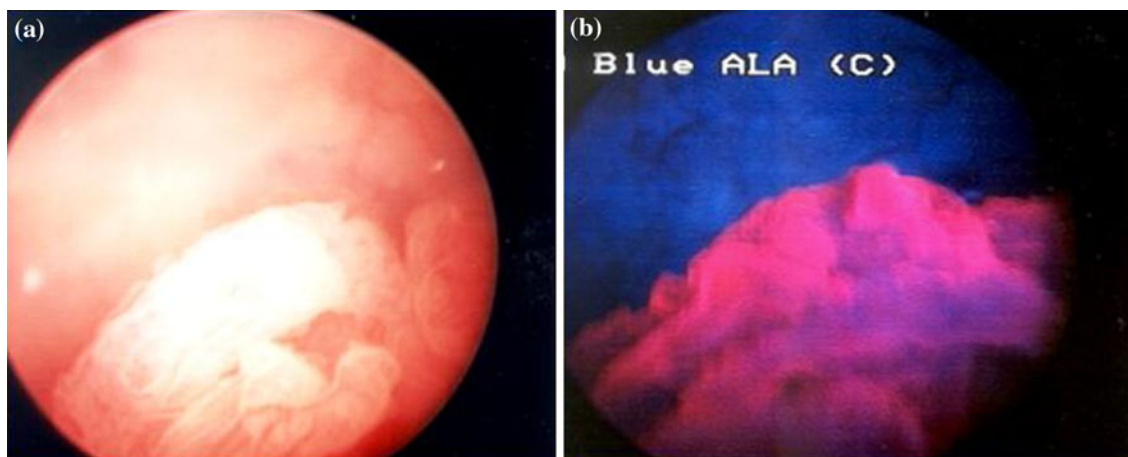

FIGURE 1. The distinct contrast between (a) white-light and (b) fluorescence endoscopic imaging of TCC after instillation with HY. The red fluorescence region in (b) indicates the presence of TCC (Reproduced with permission of *International Journal of Oncology*[66].).

FIGURE 2. Increased HY intensity from (a) normal bladder, (b) TCC grade 1, and (c) TCC grade 2 to (d) CIS when excited at 488 nm (Reproduced with permission of *International Journal of Oncology*[66].).

timely tool for routine follow-up, such as urine cytology, is highly desirable. Urine cytology is an *ex vivo* screening technique that analyzes the exfoliated bladder cells from voided urine. While this technique is suitably used for detecting CIS, it has low sensitivity in identifying early or low grade bladder cancer.[18,65] Olivo *et al.*[65] has therefore undertaken a pilot study of using *ex vivo* fluorescence cytology for detecting early bladder cancer. Similar study has been demonstrated using 5-ALA, but such diagnosis required urine collection following instillation of 5-ALA in bladder of patients.[86] On the other hand, we have demonstrated a biopsy-free screening technique that combines the advantages of PDD and urine cytology even without the need for intravesical instillation of HY. In brief, the urine samples were processed to extract the exfoliated bladder cells before incubating the cells with HY solution for a fixed duration of time. A LCM (Carl Zeiss, LSM 510) coupled with a spectrometer was used to quantify the fluorescence intensity of the HY-treated cells excited at 488 nm. In line with the *in vitro* cell lines studies,[66] the exfoliated abnormal bladder cells exhibited stronger HY fluorescence compared to normal bladder cells, as shown in Fig. 3. Subsequently, Fu *et al.*[18] extended the fluorescence urine cytology by expanding the sample size and automating the fluorescence analysis of each single cell. Advanced image processing techniques were implemented to first single out bladder cells for image analysis and to eliminate the signals from other urinary components such as red blood cells and crystalline contaminants. The intensity histograms were then extracted from the processed images and the first three moments were derived to represent the image data. Figure 3 depicts the different histogram profiles of the urothelial cells. Subsequently, Bayes classification technique was carried out to classify targeted cells based on the derived moments. The results showed that the discrimination between benign cells and low-grade tumor cells is very promising, with sensitivity and specificity above 90%. Furthermore, its diagnostic performance is found to surpass that of conventional urine cytology. To this end, the findings
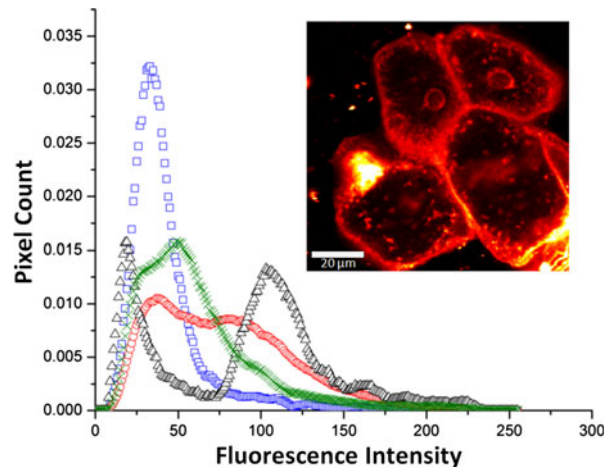
FIGURE 3. Typical histogram data from the processed fluorescence images of normal (□), low-grade tumor (○), high-grade tumor (Δ), and inflammatory (×) bladder classes. (Reproduced with permission of *International Journal of Oncology*[18].) Inset shows the typical image of TCC urothelial cells obtained with fluorescence urine cytology (Reproduced with permission of *International Journal of Oncology*[65].).

suggest that the *ex vivo* fluorescence urine cytology using HY provide a non-invasive means of detecting the early bladder cancer.

Fluorescence Endoscopy

Currently, oral cancer and bladder cancer are diagnosed by examination under WLE followed by random biopsies on suspicious-looking tissues and histological examination of the biopsies. Histopathological examination of biopsy tissue remains the gold standard for definitive diagnosis. However, this approach to make diagnosis presents at least two key limitations. First, early flat oral or bladder lesions are hardly visible, and it is difficult to distinguish between benign and early cancer.[9,88] Poor visual contrast in WLE therefore necessitates a random sampling of tissues, but still risks missing the lesion and gives false negative results.[3] Additional biopsies could also cause unnecessary suffering to patients. Needless to say, a complete surgical clearance would also be difficult. Second, tissue processing is

laborious and dependent on the skill of the operator. The histopathological examination also relies on subjective visual impression from clinicians. It is therefore of interest to develop novel imaging techniques that can provide objective and accurate diagnosis without the need for tissue resection.

Following the earlier statement that PSs accumulate selectively in abnormal cells, the microscopic fluorescence analysis was extended to macroscopic endoscopic images. FE was used to highlight lesions from which the PS fluorescence is emitted when excited by light at appropriate wavelength. Several groups have explored PSs that were suitably used in fluorescence endoscopy in an attempt to overcome the shortcomings of WLE.[73,80,106,112] To date, a number of review articles are available to compare the efficacy of different PSs for detecting bladder tumor.[33,34,44,60] A comparison of their diagnostic performance is thus not reviewed here. In essence, the mean value of the sensitivity for FE is 93% compared to only 73% for WLE.[34] The increase in diagnostic sensitivity (82% for HY vs. 62% for white-light) compared to WLE has led to use of HY in fluorescence-guided biopsies to minimize unnecessary biopsies.[81]

Fluorescence endoscope is often merged with the existing WLE system that facilitates clinicians to position the imaging probe and to sample the tissue for any further diagnosis.[107] Figure 4a depicts a typical FE system (Karl Storz Endoscope, Germany) that was custom-built to directly visualize lesions after intravesical instillation of HY for routine diagnosis as well as surgical procedures.[88,112] Ideally, a FE system was designed to irradiate the PS with excitation filter chosen to exactly match its absorption peak. Subsequently, the

resulting fluorescence emission was specifically filtered for sole detection of PS fluorescence. The imaging system in Fig. 4a was equipped with a xenon short arc lamp for white-illumination. HY fluorescence was induced when the excitation light was filtered by a bandpass filter (380–440 nm), whereas the emitted fluorescence signal was filtered by a long-pass (LP) filter (cut-off wavelength at 480 nm) before reaching the CCD camera. This observation LP filter transmitted 8% of the backscattered excitation light at 450 nm, while it had a transmission of over 98% in the 470–800 nm. The marginal detection of the excitation light was in fact useful to eliminate variations due to day-to-day intensity fluctuations of the excitation source and to calibrate the probe-to-tissue distance.[112] The endoscopy was finally interfaced to a PC for image acquisition and final analysis.

The acquired fluorescence images were first pre-processed to extract the region-of-interest (ROI) or the approximated region of lesion based on hue thresholding, as shown in Figs. 4b and 4c. The calculated hue histogram showed a bimodal distribution, with two peaks indicating the fluorescence characteristics of HY and healthy tissue, respectively. In relation to the preferential accumulation of HY in tumor, hue thresholding at global minimum was found to be effective in estimating the tumor margin.[39] Diagnostic parameters of the segmented images, i.e., the ROIs, were then extracted and expressed in terms of the red (I_R), green (I_G), and blue (I_B) intensity values (RGB), as well as the hue, saturation, and intensity (HSI) values.[88,107] The result showed that the red-to-blue intensity ratio (I_R/I_B) was the best image parameter for discriminating normal from hyperplastic tissues with the sensitivity
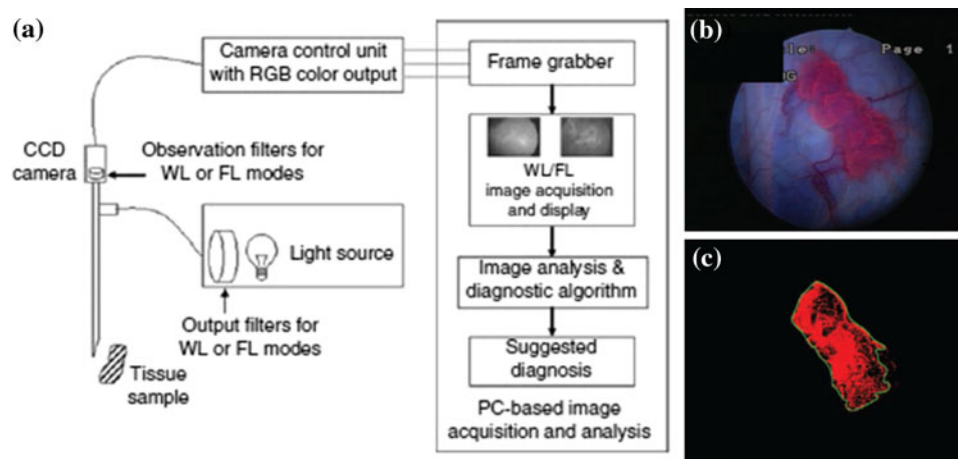
FIGURE 4. (a) A fluorescence endoscopy system interfaced to a PC-based image acquisition and analysis system for fluorescence diagnostic imaging. (Reproduced with permission of *British Journal of Cancer*[88].) (b) Under blue-light excitation, the autofluorescence of healthy tissue and HY fluorescence of cancerous tissue can be clearly discerned. (c) The system is also capable of defining the AOI where the tumor is localized for fluorescence analysis (Reproduced with permission of *Lasers in Surgery and Medicine*[39].).

and specificity of 100 and 96%, respectively; normal from squamous-cell carcinoma (SCC) tissues with sensitivity and specificity of 100%, respectively; and hyperplastic from SCC with 92 and 90%, respectively.[88] The discerning of normal tissue from hyperplastic and the SCC tissues by difference in red-to-blue intensity (I_R/I_B) as in Fig. 5. The I_R corresponded to the HY fluorescence intensity, indicating a selective uptake amount of HY in lesions; on the other hand, the backscattered blue excitation light contributed to the I_B. Furthermore, the diagnostic accuracy could be elevated by multivariate analysis. For instance, combining the two ratio diagnostic algorithms (I_R/I_G vs. I_R/I_B) was shown to yield diagnostic accuracy exceeding those from each diagnostic algorithm alone.[112] Using a high-speed computing platform, a prototype of the real-time imager was developed to automate delineation of ROI, system calibration and immediate tissue classification based on previously developed algorithms. This integrated system thus not only provided a diagnostic prediction and immediate feedback for clinicians, but also offered surgeons a visual aid for demarcation of tumor margin needed in a precise surgical resection.[88]

Real-Time 3D Endomicroscopy

To take this HY-mediated fluorescence endoscopy platform further, our group developed an embedded, real-time computing system interfaced with a confocal laser endomicroscopy (CLE) for 3D visualization of tumors.[90] CLE has been applied for autofluorescence diagnostic imaging in gastroenterology,[20,29,46,71] gynecology,[85] urology,[83] human oral, and oropharyngeal mucosa.[23] A CLE offers imaging capabilities for *in vivo* fluorescence imaging of tissue structures from the surface to a few hundred micrometers beneath the surface.[17,46] This sub-surface imaging has been found useful to detect malignancy by means of the altered tissue architecture and irregularities in blood vessels.[23]

Figure 6a illustrates the setup of a CLE (Optiscan, Australia) that encompasses the 488-nm-laser, optical filters, and lenses to image HY-fluorescence from the tissues. Similar setup was also reported by D'Hallewin *et al.*,[13] for detecting the differences in fluorescence intensity and morphology of the epithelial cells. The single-mode fiber enclosed in the rigid probe was movable to collect fluorescence signal at different focal planes, thereby capable of probing HY amount as a function of tissue depth. Images were acquired with a field of view of 475 by 475 μm and a lateral resolution of 0.7 μm. The image depth was about 250 μm, depending on scattering and absorption properties of tissue under investigation. Consecutive images of a murine tongue were acquired at different tissue layers following topical application of HY (see Fig. 6b). We have further developed CLE by interfacing the probe to a high-performance computing system.[10] This prototype enabled a real-time 3D fluorescence visualization realized through programming a Field-Programmable Gate Array (RC340 FPGA, Mentor Graphics Corporation, USA) board. The 3D visualization of a tissue
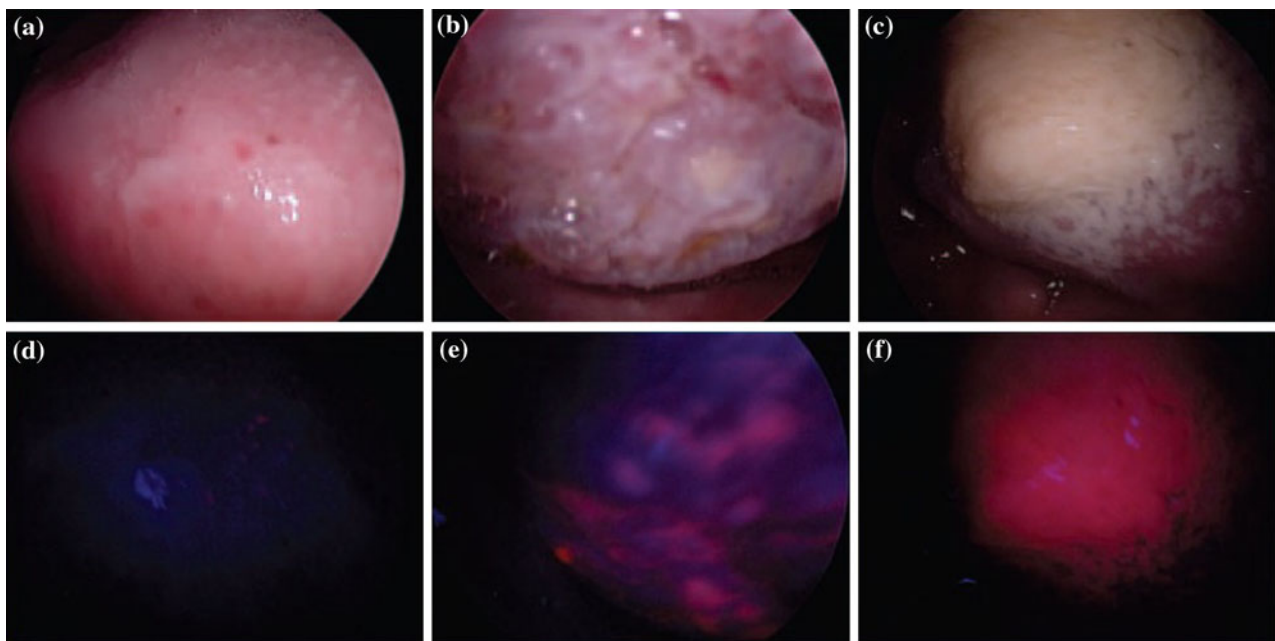
FIGURE 5. White-light and HY-induced fluorescence images of normal (a, d), hyperplastic (b, e) and SCC tissues (c, f). Progressive increase in I_R/I_B ratio can be seen from normal to hyperplastic to SCC lesions (Reproduced with permission of *British Journal of Cancer*[88].).
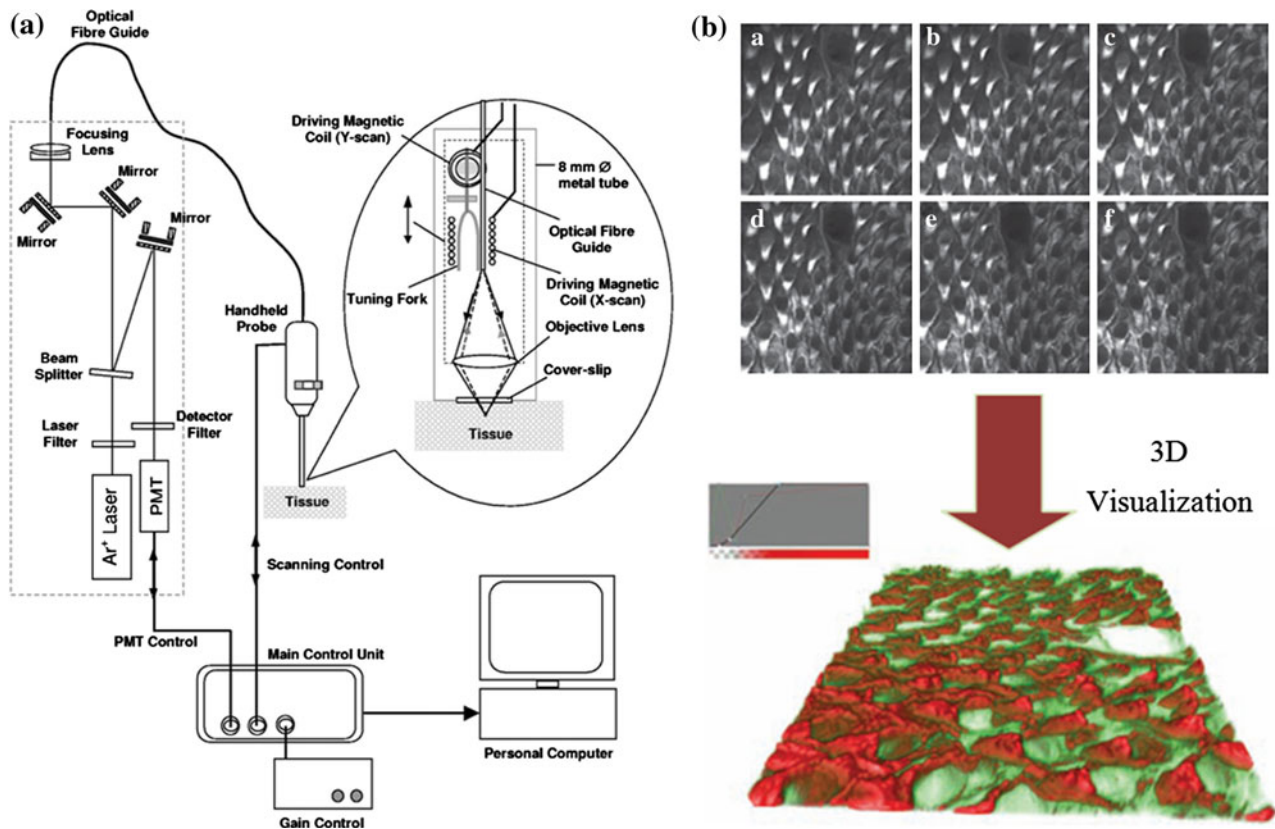
FIGURE 6. (a) An endomicroscope interfaced with a Field Programmable Gated Array (FGPA) board designed for automated real-time 3D imaging and reconstruction of fluorescent samples. The movable single-mode fiber enclosed in the handheld probe was used to collect fluorescence signal emitted from different tissue depths. (Reproduced with permission of *Journal of Biomedical Optics*[89].) (b) Six consecutive images were measured from different depths of the murine tongue following topical application of HY. A 3D image was later reconstructed from those images and was displayed in pseudo-color (Reproduced with permission of *Journal of Medical Imaging and Health Informatics*[91].).

can be reconstructed from a stack of fluorescence images acquired as demonstrated in Fig. 6b.[91] The results showed that distinct 3D structures in the murine tongue can be visualized and demonstrated the potential of 3D endomicroscopy for diagnostic imaging of the oral cavity. Unlike the aforementioned fluorescence endoscopy, this approach gives additional diagnostic information about the tissue structure. With the 3D diagnostic images, the HY fluorescence signals can be fully used to enhance the morphological differences between normal and diseased tissue. Likewise, it is possible to examine the blood vessel architecture that is associated with cancer development. However, extraneous light absorption and scattering from turbid tissue is always inevitable, and a proper recovery of fluorescence signal is thus necessary to accurately quantify the concentration of HY. For instance, Xie *et al.*[99] have presented the use of Monte Carlo simulation to effectively compensate the light-attenuation for corrected fluorescence images. We thus anticipate that a real-time 3D endomicroscopy system coupled with recovery algorithm can complement WLE and FE in a clinical setting by providing the morphological details.

COUPLING WITH NANOTECHNOLOGY FOR COMBINATORIAL THERAPEUTIC AND MULTIMODALITY IMAGING

Traditionally, PSs are solely used for PDT in cancer treatment, and their inherent fluorescence properties are utilized to aid diagnosis as discussed in previous section. However, the recent advancements in nanotechnology opens up new horizon for PSs to be applied in entirely different ways. A short review is presented here to highlight the possibility of developing nanoconstruct integrated with HY for combinatorial therapeutic and multimodality imaging.

Enhanced Targeted Delivery

As with most PSs, HY has limited water solubility that makes systemic administration problematic and, in turn, affects its delivery to and uptake by tumor cells.[50,52] Many efforts are ongoing to formulate better PSs, but the pharmaceutical preparation is difficult,[7] and issues associated with dark cytotoxicity and deficient *in vivo* selectivity are yet to be solved.[72] This has

led to the development of third-generation PSs that are now equipped with nanocarrier systems to enhance their targeted delivery for efficient PDT and PDD.[35] These nanocarriers, which load PSs by adsorption or covalent binding, offer benefits of hydrophilicity and appropriate size for passive targeting of tumor by the enhanced permeability and retention (EPR) effect.[7] To enhance accumulation, instead of reformulating the PSs, the surface of carriers is functionalized for active receptor-mediated targeting. Various types of nanocarriers are available and their use in PDT has been extensively reviewed. In particular, gold nanoparticles (GNPs), such as spherical gold nanoparticles (SGNPs)[61,67] and gold nanorod (GNRs),[53,96,105] are in favor as PS carriers due to their biocompatibility, easy preparation, efficient bioconjugation, and high-drug loading capacity.[25] GNPs are usually shielded with polyethylene glycol (PEG) for prolonged circulation time in the body.[63] Such GNPs are thus ideal platform for delivering hydrophobic HY to tumor site, with minimal damage to the normal tissue (See Fig. 7a).[2,84,104] For instance, anti-EGFR-labeled HY-SGNP was used to target EGFR-overexpressing A-431 cancer cell lines.[67] Figure 7b depicts the strong yellowish light scattering of HY-SGNP as observed under a dark-field microscopy, confirming localization of particles at the cell surface via receptor-mediated cell targeting. The fluorescence studies also suggested that the *in vitro* uptake of HY-SGNP is comparable to HY alone (see Fig. 7b). However, in this case, the fluorescence intensity measured from the nanosensitizer may not truly represent the uptake quantity due to a possible fluorescence quenching of hypercin molecules close to the SGNPs.[79] Ongoing studies are underway to optimize the loading of HY onto the nanoconstruct for enhanced PDD.
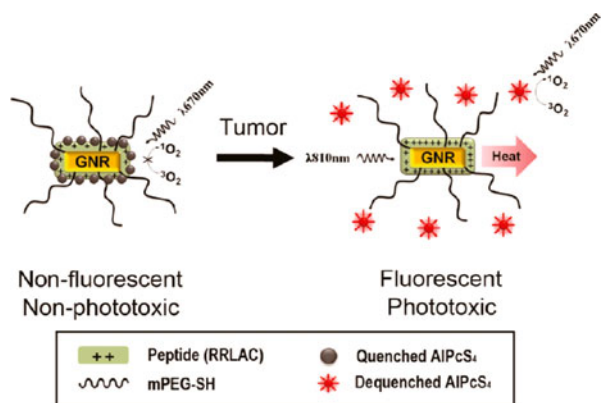
Photothermal Therapy

Nanometer-sized gold particles are known to exhibit surface plasmon resonance (SPR) effect that is absent in bulk gold. This plasmonic feature makes GNPs efficient in generating heat in the presence of electromagnetic radiation.[21] At SPR frequency, the strongly absorbed radiation is converted into heat by electron–phonon and phonon–phonon processes.[26] The particles thus serve as heating elements that lead to elevated temperature of the surrounding medium and induce hyperthermia or irreversible thermal damage to the targeted tissue, thereby offering an alternative cancer treatment called photothermal therapy (PTT).[32,95] A study showed that the heat conversion efficiency of GNPs increases with their size.[21] In addition, aspect ratio of the GNRs can be tailored to operate PTT within the optical window between 700 and 900 nm, where light penetration in tissue is optimal due to minimal absorption by water and hemoglobin in the tissue[95]; consequently, the excitation light can reach deeper tissues and induce PTT. More importantly, recent studies suggest that PDT and PTT can potentially be merged for efficient cancer treatment.[31,41,67]

Controlled Drug Release for PDT

The photothermal heating can further be exploited to release drug that is loaded onto the GNPs. Photo-activated release of PS was demonstrated using a GNR–PS complex as elucidated in Fig. 8.[31] Initially, GNRs quench the fluorescence emission of PS molecules that are in close proximity (< 40 nm)[22] to the gold surface due to efficient energy transfer from PSs to GNRs. When irradiated at 810 nm, the photothermal heating generated by GNRs liberates the PS from
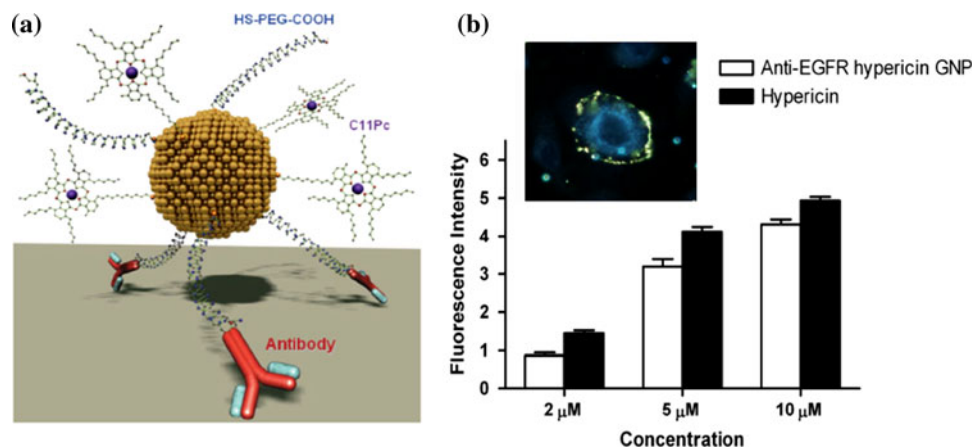
FIGURE 7. (a) Illustration of a nanoconstruct consists of PS molecules (C11PC) for PDT, PEG for increased stability, and antibody for cancer-targeting. (Reproduced with permission of *Photochemical & Photobiological Sciences*[84].) (b) Comparison of HY fluorescence intensity in A-431 cells following incubation with anti-EGFR conjugated HY-SGNP and HY alone. The inset shows the dark-field images of the cells targeted by the particles. (Reproduced with permission of *SPIE Proceedings*[67].)

FIGURE 8. Illustration of photo-activated release of PS (AlPcS$_4$). PDT is prohibited before photothermal heating of GNR. Irradiation at 810 nm results in photothermal heating that releases PS from the GNR. The liberated PS molecules thereafter undergo PDT action in response to excitation at 670 nm (Reproduced with permission of *ACS Nano*[31].).

the surface to undergo PDT in response to a second excitation at 670 nm. The PDT efficacy can thus be photothermally controlled by manipulating the distance between the PSs and GNRs.

Multimodality Imaging

There are other features of gold nanostructures that are worthy of mention. These gold nanostructures often possess high scattering cross sections and are able to enhance the weak Raman signal of molecules. Though HY fluorescence is more commonly studied, its Raman characteristics should not be ignored as the Raman signal is detectable when the HY molecules are sufficiently close to the gold surface which induces surface-enhanced Raman scattering (SERS).[24] A study has shown that a joint fluorescence and SERS measurement of HY can facilitate the understanding of its biological activity.[54]

While PSs are useful in giving molecular contrast in fluorescence and SERS imaging, the gold nanostructures serve as additional optical contrast agent in other structural imaging such as optical coherence tomography (OCT)[27] and two-photon luminescence.[113] In particular, OCT, a biopsy-free imaging, is being used for *in vivo* clinical applications.[5,19,57] The advantage of OCT is its ability to provide cross-sectional images of tissue with high spatial resolution by measuring the optical echoes backscattered from tissue.[27] Currently, much effort is put to further develop OCT toward acquisition of histologically equivalent images for definitive diagnosis without the need of biopsies. The contrast in OCT image is highly dependent on the microscopic differences in scattering properties across the tissue layers. However, the early onset of tissue abnormalities barely changes the tissue optics that

result in poor morphological contrast between normal and abnormal tissues in OCT images.[38,40] To overcome these limitations, gold nanostructures, along with being utilized as a PS carrier, are used to increase the diagnostic and analytic capabilities of OCT by site-specific labeling of tissue of interest. The plasmonically active nanostructures, such as GNPs,[40,48] GNRs,[92] nanoshell[55], and nanocages,[8] can be optically tuned to specifically scatter the OCT probe beam. The key idea is simply to use OCT to demarcate the abnormal sites at which these light-scattering particles are targeted. Though this concept was demonstrated using rigid OCT probe, there are several groups[1,36,47,110] working on miniaturization of OCT system that can potentially be merged with existing fluorescence endoscopy. For example, Mu *et al.*[98] have developed a microelectromechanical systems (MEMS)-based OCT catheters to perform a rapid 3D volumetric scanning. This MEMS-OCT probe has an outer diameter of only 4 mm and encloses a patented MEMS micromirror as the optical steerer. One can envision that such technique combined with molecular imaging is powerful for improved diagnosis and informative monitoring of tissue structures during PDT or PTT. Hence, combining advancements in PDD and nanotechnology offers the opportunity to significantly impact future strategies toward improved multimodality therapeutics and imaging.

CONCLUSION

We have investigated the combined use of HY and state-of-the-art optical techniques for detecting early cancer, with improved diagnostic accuracy in comparison with the standard clinical practice. The standard diagnosis, which relies on WLE, lacks the ability in identifying early and flat lesions, and thus runs the risk of giving false negative results. HY used with novel optical techniques provides an alternative to detect the subtle structural and molecular changes expressed during the development of cancer.

We began by discussing the increased uptake of HY in progressively invasive cancer cell lines and biopsies. The tumor selectivity of HY, especially in bladder cancer, makes it a suitable fluorescent contrast agent in differentiating the scattered cancerous sites from the surrounding healthy tissues. These fluorescence properties were first exploited in *ex vivo* fluorescence urine cytology. Unlike tissue sampling, the cell yield in urine cytology is rather limited, and the presence of contaminants in urine could complicate the fluorescence analysis. Image processing techniques were applied to get around the problem. Meanwhile, the diagnostic information from each single cell was also maximized

by studying the HY intensity histogram. Subsequently, the microscopic diagnosis with HY was extended to macroscopic level using FE. FE was employed to diagnose bladder and oral cavity *in situ*. With the use of appropriate camera and optics elements, a single shot of fluorescence image was adequate to perform a real-time PDD without the need for a slow fluorescence spectral measurement. Fluorescence diagnosis could be automated and visual aid was provided to clinicians for a fluorescence-guided biopsy or resection of tumor. PDD was further developed by incorporating a CLE for probing the HY intensity at different tissue depths. In addition, fluorescence images collected at different focal planes were processed to render a 3D visualization from which more detailed information about the lesion morphology could be assessed.

While the fluorescence properties of the HY have been well exploited in PDD, we discuss about the underlying trend of coupling HY with the nanotechnology for combined therapeutics and multimodality imaging. The use of gold nanostructures not only enhances the targeted delivery of HY to cancer cells, but also serves as a heating element to trigger PTT as well as providing optical contrast for other optical imaging techniques. Meanwhile, the photoheating of GNPs was utilized to manage the release of HY from nanoconstruct, thus controlling the PDT efficacy; such approach may carry high potential for modulating PDT and PTT. Apart from enhancing molecular contrast with HY, the nanoparticles serve as complimentary contrast agent when used with other novel optical imaging modalities, such as two-photon luminescence imaging, dark-field microscopy, OCT, and SERS. With the continual effort in this field, we envision a successful integration of PSs and multifunctional nanoparticles to realize informative diagnosis followed by a multifaceted therapy in near future.

OPEN ACCESS

REFERENCES

[1] Aljasem, K., A. Werber, A. Seifert, and H. Zappe. Fiber optic tunable probe for endoscopic optical coherence tomography. *J. Opt. A Pure Appl. Opt.* 10:044012, 2008.

[2] Bechet, D., P. Couleaud, C. Frochot, M. Viriot, F. Guillemin, and M. Barberi-Heyob. Nanoparticles as vehicles for delivery of photodynamic therapy agents. *Trends Biotechnol.* 26(11):612–621, 2008.

[3] Benaron, D. The future of cancer imaging. *Cancer Metastasis Rev.* 21(1):45–78, 2002.

[4] Benavides, J., S. Chang, S. Park, R. Richards-Kortum, N. Mackinnon, C. Macaulay, A. Milbourne, A. Malpica, and M. Follen. Multispectral digital colposcopy for in vivo detection of cervical cancer. *Opt. Express* 11(10):1223–1236, 2003.

[5] Boppart, S., B. Bouma, C. Pitris, J. Southern, M. Brezinski, and J. Fujimoto. In vivo cellular optical coherence tomography imaging. *Nat. Med.* 4(7):861–865, 1998.

[6] Castano, A., T. Demidova, and M. Hamblin. Mechanisms in photodynamic therapy: part one? Photosensitizers, photochemistry and cellular localization. *Photodiagn. Photodyn. Ther.* 1(4):279–293, 2004.

[7] Chatterjee, D. K., L. S. Fong, and Y. Zhang. Nanoparticles in photodynamic therapy: an emerging paradigm. *Adv. Drug Deliv. Rev.* 60(15):1627–1637, 2008.

[8] Chen, J., F. Saeki, B. Wiley, H. Cang, M. Cobb, Z. Li, L. Au, H. Zhang, M. Kimmey, X. Li, and Y. Xia. Gold nanocages: bioconjugation and their potential use as optical imaging contrast agents. *Nano Lett.* 5(3):473–477, 2005.

[9] Cheng, C., W. Lau, P. Tan, and M. Olivo. Cystoscopic diagnosis of bladder cancer by intravesical instillation of 5-aminolevulinic acid induced porphyrin fluorescence—the singapore experience. *Ann. Acad. Med. Singap.* 29(2):153–158, 2000.

[10] Cheong, L. S., F. Lin, H. S. Seah, K. Qian, F. Zhao, P. S. P. Thong, K. C. Soo, M. Olivo, and S. Y. Kung. Embedded computing for fluorescence confocal endomicroscopy imaging (1). *J. Signal Process. Syst.* 55(1–3):217–228, 2009.

[11] D'Hallewin, M., L. Bezdetnaya, and F. Guillemin. Fluorescence detection of bladder cancer: a review. *Eur. Urol.* 42(5):417–425, 2002.

[12] D'Hallewin, M., P. de Witte, E. Waelkens, W. Merlevede, and L. Baert. Fluorescence detection of flat bladder carcinoma in situ after intravesical instillation of hypericin. *J. Urol.* 164(2):349–351, 2000.

[13] D'Hallewin, M., K. El Khatib, A. Leroux, L. Bezdetnaya, and F. Guillemin. Endoscopic confocal fluorescence microscopy of normal and tumor bearing rat bladder. *J. Urol.* 174(2):736–740, 2005.

[14] D'Hallewin, M., A. Kamuhabwa, T. Roskams, P. De Witte, and L. Baert. Hypericin-based fluorescence diagnosis of bladder carcinoma. *BJU Int.* 89(7):760, 2002.

[15] Dets, S. M., A. N. Buryi, I. S. Melnik, A. Y. Joffe, and T. V. Rusina. Laser-induced fluorescence detection of stomach cancer using hypericin. *SPIE Proc.* 2926:51–56, 1996.

[16] Dolmans, D., and R. D. Fukumura. Photodynamic therapy for cancer. *Nat. Rev. Cancer* 3(5):380, 2003.

[17] Flusberg, B., E. Cocker, W. Piyawattanametha, J. Jung, E. Cheung, and M. Schnitzer. Fiber-optic fluorescence imaging. *Nat. Methods* 2(12):941–950, 2005.

[18] Fu, C., B. Ng, and S. Razul. Fluorescence detection of bladder cancer using urine cytology. *Int. J. Oncol.* 31(3):525–530, 2007.

[19] Fujimoto, J. G., C. Pitris, S. A. Boppart, and M. E. Brezinski. Optical coherence tomography an emerging technology for biomedical imaging and optical biopsy. *Neoplasia* 2(1–2):9–25, 2000.

[20]Goetz, M., and R. Kiesslich. Advances of endomicroscopy for gastrointestinal physiology and diseases. *Am. J. Physiol. Gastrointest. Liver Physiol.* 298(6):G797–G806, 2010.

[21]Govorov, A. O., and H. Richardson. Generating heat with metal nanoparticles. *NanoToday* 2(1):20–39, 2007.

[22]Griffin, J., A. Singh, D. Senapati, P. Rhodes, K. Mitchell, B. Robinson, E. Yu, and P. Ray. Size- and distance-dependent nanoparticle surface-energy transfer (NSET) method for selective sensing of hepatitis c virus RNA. *Chemistry* 15(2):342–351, 2009.

[23]Haxel, B. R., M. Goetz, R. Kiesslich, and J. Gosepath. Confocal endomicroscopy: a novel application for imaging of oral and oropharyngeal mucosa in human. *Eur. Arch. Otorhinolaryngol.* 267(3):443–448, 2010.

[24]Haynes, C. L., A. D. McFarland, and R. P. V. Duyne. Surface-enhanced raman spectroscopy. *Anal. Chem.* 77(17):338A–346A, 2005.

[25]Huang, X., P. Jain, I. El-Sayed, and M. El-Sayed. Gold nanoparticles: interesting optical properties and recent applications in cancer diagnostics and therapy. *Nanomedicine (Lond.)* 2(5):681–693, 2007.

[26]Huang, X., S. Neretina, and M. A. El-Sayed. Gold nanorods: from synthesis and properties to biological and biomedical applications. *Adv. Mater.* 21(48):4880–4910, 2009.

[27]Huang, D., E. Swanson, C. Lin, J. Schuman, W. Stinson, W. Chang, M. Hee, T. Flotte, K. Gregory, C. Puliafito, and J. Fujimoto. Optical coherence tomography. *Science* 254(5035):1178–1181, 1991.

[28]Huang, Z., S. K. Teh, W. Zheng, J. Mo, K. Lin, X. Shao, K. Y. Ho, M. Teh, and K. G. Yeoh. Integrated Raman spectroscopy and trimodal wide-field imaging techniques for real-time in vivo tissue raman measurements at endoscopy. *Opt. Lett.* 34(6):758–760, 2009.

[29]Hurlstone, D., W. Baraza, S. Brown, M. Thomson, N. Tiffin, and S. Cross. In vivo real-time confocal laser scanning endomicroscopic colonoscopy for the detection and characterization of colorectal neoplasia. *Br. J. Surg.* 95(5):636–645, 2008.

[30]Huygens, A., A. Kamuhabwa, T. Roskams, C. Van, P. Van, and W. de Witte. Permeation of hypericin in spheroids composed of different grade transitional cell carcinoma cell lines and normal human urothelial cells. *J. Urol.* 174(1):69–72, 2005.

[31]Jang, B., J. Y. Park, C. H. Tung, I. H. Kim, and Y. Choi. Gold nanorod–photosensitizer complex for near-infrared fluorescence imaging and photodynamic/photothermal therapy in vivo. *ACS Nano* 5(2):1086–1094, 2011.

[32]Jelveh, S., and D. B. Chithrani. Gold nanostructures as a platform for combinational therapy in future cancer therapeutics. *Cancers* 3(1):1081–1110, 2011.

[33]Jichlinski, P., and D. Jacqmin. Photodynamic diagnosis in non-muscle-invasive bladder cancer. *Eur. Urol. Suppl.* 7(7):529–535, 2008.

[34]Jocham, D., H. Stepp, and R. Waidelich. Photodynamic diagnosis in urology: state-of-the-art (1). *Eur. Urol.* 53(6):1138–1150, 2008.

[35]Josefsen, L. B., and R. W. Boyle. Photodynamic therapy novel third-generation photosensitizers one step closer. *Br. J. Pharmacol.* 154(1):1–3, 2008.

[36]Jung, W., D. McCormick, J. Zhang, L. Wang, N. Tien, and Z. Chen. Three-dimensional endoscopic optical coherence tomography by use of a two-axis microelectromechanical scanning mirror. *Appl. Phys. Lett.* 88:163901, 2006.

[37]Juzeniene, A., Q. Peng, and J. Moan. Milestones in the development of photodynamic therapy and fluorescence diagnosis. *Photochem. Photobiol. Sci.* 6(12):1234–1245, 2007.

[38]Kah, J., T. Chow, B. Ng, S. Razul, M. Olivo, and C. Sheppard. Concentration dependence of gold nanoshells on the enhancement of optical coherence tomography images: a quantitative study. *Appl. Opt.* 48(10):D96–D108, 2009.

[39]Kah, J. C. Y., W. K. O. Lau, P. H. Tan, C. J. R. Sheppard, and M. Olivo. Endoscopic image analysis of photosensitizer fluorescence as a promising noninvasive approach for pathological grading of bladder cancer in situ. *J. Biomed. Opt.* 13(5):054022, 2008.

[40]Kah, J., M. Olivo, T. Chow, K. Song, K. Koh, S. Mhaisalkar, and C. Sheppard. Control of optical contrast using gold nanoshells for optical coherence tomography imaging of mouse xenograft tumor model in vivo. *J. Biomed. Opt.* 14(5):054015, 2009.

[41]Kah, J. C. Y., R. C. Y. Wan, K. Y. Wong, S. Mhaisalkar, C. J. R. Sheppard, and M. Olivo. Combinatorial treatment of photothermal therapy using gold nanoshells with conventional photodynamic therapy to improve treatment efficacy: an in vitro study. *Lasers Surg. Med.* 40(8):584–589, 2008.

[42]Kamuhabwa, A., R. Roelandts, and W. de Witte. Skin photosensitization with topical hypericin in hairless mice. *J. Photochem. Photobiol. B* 53(1–3):110–114, 1999.

[43]Kamuhabwa, A., T. Roskams, L. Baert, and W. de Witte. Microscopic quantification of hypercin fluorescence in an orthotopic rat bladder tumor model after intravesical instillation. *Int. J. Oncol.* 22(4):933–937, 2003.

[44]Kausch, I., M. Sommerauer, F. Montorsi, A. Stenzl, D. Jacqmin, P. Jichlinski, D. Jocham, A. Ziegler, and R. Vonthein. Photodynamic diagnosis in non-muscle-invasive bladder cancer: a systematic review and cumulative analysis of prospective studies. *Eur. Urol.* 57(4):595–606, 2010.

[45]Kennedy, J., R. Pottier, and D. Pross. Photodynamic therapy with endogenous protoporphyrin IX: basic principles and present clinical experience. *J. Photochem. Photobiol. B* 6(1–2):143–148, 1990.

[46]Kiesslich, R., and M. Canto. Confocal laser endomicroscopy. *Gastrointest. Endosc. Clin. N. Am.* 19(2):261–272, 2009.

[47]Kim, K., B. Park, G. Maguluri, T. Lee, F. Rogomentich, M. Bancu, B. Bouma, B. de Boer, and J. Bernstein. Two-axis magnetically-driven MEMS scanning catheter for endoscopic high-speed optical coherence tomography. *Opt. Express* 15(26):18130–18140, 2007.

[48]Kim, C. S., P. Wilder-Smith, Y. C. Ahn, L. H. L. Liaw, Z. Chen, and Y. J. Kwon. Enhanced detection of early-stage oral cancer in vivo by optical coherence tomography using multimodal delivery of gold nanoparticles. *J. Biomed. Opt.* 14(3):034008, 2009.

[49]Koenig, F., F. McGovern, A. Althausen, T. Deutsch, and K. Schomacker. Laser induced autofluorescence diagnosis of bladder cancer. *J. Urol.* 156(5):1597–1601, 1996.

[50]Konan, Y., R. Gurny, and E. Allmann. State of the art in the delivery of photosensitizers for photodynamic therapy. *J. Photochem. Photobiol. B* 66(2):89, 2002.

[51]Kraft, M., C. S. Betz, A. Leunig, and C. Arens. Value of fluorescence endoscopy for the early diagnosis of laryngeal cancer and its precursor lesions. *Head Neck* 33(7):941–948, 2011.

[52]Kubin, A., F. Wierrani, U. Burner, G. Alth, and W. Grunberger. Hypericin-the facts about a controversial agent. *Curr. Pharm. Des.* 11(2):233, 2005.

[53]Kuo, W. S., C. N. Chang, Y. T. Chang, M. H. Yang, Y. H. Chien, S. J. Chen, and C. S. Yeh. Near-infrared Au nanorods in photodynamic therapy, hyperthermia agents, and near-infrared optical imaging. *Proc. SPIE.* 7910: 791009, 2011.

[54]Lajos, G., D. Jancura, P. Miskovsky, J. V. Garca-Ramos, and S. Sanchez-Cortes. Surface-enhanced fluorescence and raman scattering study of antitumoral drug hypericin: an effect of aggregation and self-spacing depending on pH. *J. Phys. Chem. C* 112(33):12974–12980, 2008.

[55]Loo, C., A. Lin, L. Hirsch, M. Lee, J. Barton, N. Halas, J. West, and R. Drezek. Nanoshell-enabled photonics-based imaging and therapy of cancer. *Technol. Cancer Res. Treat.* 3(1):33–40, 2004.

[56]Mang, T., J. Kost, M. Sullivan, and B. Wilson. Autofluorescence and photofrin-induced fluorescence imaging and spectroscopy in an animal model of oral cancer. *Photodiagn. Photodyn. Ther.* 3(3):168–176, 2006.

[57]Matheny, E., N. Hanna, W. Jung, Z. Chen, P. Wilder-Smith, R. Mina-Araghi, and M. Brenner. Optical coherence tomography of malignancy in hamster cheek pouches. *J. Biomed. Opt.* 9(5):978–981, 2004.

[58]Melnik, I., S. Dets, T. Rusina, N. Denisov, E. Braun, V. Kikot, and V. Chernyj. Accumulation of hypericin in human gastric tumors. *SPIE Proc.* 2675:67, 1996.

[59]Mycek, M. A., and B. W. Pogue. Handbook of Biomedical Fluorescence. New York: Marcel Dekker, 665 pp, 2003.

[60]O'Brien, T., and K. Thomas. Bladder cancer: photodynamic diagnosis can improve surgical outcome. *Nat. Rev. Urol.* 7(11):598, 2010.

[61]O'Neal, D., L. R. Hirsch, N. J. Halas, J. Payne, and J. L. West. Photo-thermal tumor ablation in mice using near infrared-absorbing nanoparticles. *Cancer Lett.* 209(2): 171–176, 2004.

[62]Olivo, M., R. Bhuvaneswari, and I. Keogh. Advances in bio-optical imaging for the diagnosis of early oral cancer. *Pharmaceutics* 3(3):354–378, 2011.

[63]Olivo, M., R. Bhuvaneswari, S. S. Lucky, N. Dendukuri, and P. Soo-Ping Thong. Targeted therapy of cancer using photodynamic therapy in combination with multi-faceted anti-tumor modalities. *Pharmaceuticals* 3(5):1507–1529, 2010.

[64]Olivo, M., H. Du, and B. Bay. Hypericin lights up the way for the potential treatment of nasopharyngeal cancer by photodynamic therapy. *Curr. Clin. Pharmacol.* 1(3):217–222, 2006.

[65]Olivo, M., W. Lau, V. Manivasager, R. Bhuvaneswari, Z. Wei, K. C. Soo, C. Cheng, and P. H. Tan. Novel photodynamic diagnosis of bladder cancer: ex vivo fluorescence cytology using hypericin. *Int. J. Oncol.* 23(6):1501–1504, 2003.

[66]Olivo, M., W. Lau, V. Manivasager, P. H. Tan, K. C. Soo, and C. Cheng. Macro-microscopic fluorescence of human bladder cancer using hypericin fluorescence cystoscopy and laser confocal microscopy. *Int. J. Oncol.* 23(4):983–990, 2003.

[67]Olivo, M., S. S. Lucky, R. Bhuvaneswari, and N. Dendukuri. Nano-sensitizers for multi-modality optical diagnostic imaging and therapy of cancer. *SPIE Proc.* 8087:8087T, 2011.

[68]Olivo, M., S. S. Lucky, J. F. Kent Mancer, and W. K. O. Lau. Altered expression of cell adhesion molecules leads to differential uptake of hypericin in urothelial cancer. *Urol. Oncol.*, 2010.

[69]Pierce, M., D. Javier, and R. R. Kortum. Optical contrast agents and imaging systems for detection and diagnosis of cancer. *Int. J. Cancer* 123(9):1979–1990, 2008.

[70]Poh, C., L. Zhang, D. Anderson, J. Durham, P. Williams, R. Priddy, K. Berean, S. Ng, O. Tseng, C. MacAulay, and M. Rosin. Fluorescence visualization detection of field alterations in tumor margins of oral cancer patients. *Clin. Cancer Res.* 12(22):6716–6722, 2006.

[71]Polglase, A., W. McLaren, and P. Delaney. Pentax confocal endomicroscope: a novel imaging device for in vivo histology of the upper and lower gastrointestinal tract. *Expert Rev. Med. Devices* 3(5):549–556, 2006.

[72]Rai, P., S. Mallidi, X. Zheng, R. Rahmanzadeh, Y. Mir, S. Elrington, A. Khurshid, and T. Hasan. Development and applications of photo-triggered theranostic agents. *Adv. Drug Deliv. Rev.* 62(11):1094–1124, 2010.

[73]Ramaswamy, B., V. Manivasager, W. Chin, K. Soo, and M. Olivo. Photodynamic diagnosis of a human nasopharyngeal carcinoma xenograft model using the novel chlorin e6 photosensitizer fotolon. *Int. J. Oncol.* 26(6):1501–1506, 2005.

[74]Roelants, M., B. Van Cleynenbreugel, E. Lerut, H. Van Poppel, and P. A. M. de Witte. Human serum albumin as key mediator of the differential accumulation of hypericin in normal urothelial cell spheroids versus urothelial cell carcinoma spheroids. *Photochem. Photobiol. Sci.* 10(1): 151–159, 2011.

[75]Saw, C. L. L., P. W. S. Heng, and M. Olivo. Potentiation of the photodynamic action of hypericin. *J. Environ. Pathol. Toxicol. Oncol.* 27(1):23–33, 2008.

[76]Saw, C., M. Olivo, W. Chin, K. Soo, and P. Heng. Superiority of *n*-methyl pyrrolidone over albumin with hypericin for fluorescence diagnosis of human bladder cancer cells implanted in the chick chorioallantoic membrane model. *J. Photochem. Photobiol. B* 86(3):207–218, 2007.

[77]Saw, C. L. L., M. Olivo, K. C. Soo, and P. W. S. Heng. Spectroscopic characterization and photobleaching kinetics of hypericin-*n*-methyl pyrrolidone formulations. *Photochem. Photobiol. Sci.* 5(11):1018, 2006.

[78]Saw, C. L. L., M. Olivo, K. C. Soo, and P. W. S. Heng. Delivery of hypericin for photodynamic applications. *Cancer Lett.* 241(1):23–30, 2006.

[79]Schneider, G., G. Decher, N. Nerambourg, R. Praho, M. Werts, and M. Blanchard-Desce. Distance-dependent fluorescence quenching on gold nanoparticles ensheathed with layer-by-layer assembled polyelectrolytes. *Nano Lett.* 6(3):530–536, 2006.

[80]Sharwani, A., W. Jerjes, V. Salih, A. MacRobert, M. El-Maaytah, H. Khalil, and C. Hopper. Fluorescence spectroscopy combined with 5-aminolevulinic acid-induced protoporphyrin IX fluorescence in detecting oral premalignancy. *J. Photochem. Photobiol. B* 83(1):27–33, 2006.

[81]Sim, H. G., W. K. Lau, M. Olivo, P. H. Tan, and C. W. Cheng. Is photodynamic diagnosis using hypericin better than white-light cystoscopy for detecting superficial bladder carcinoma? *BJU Int.* 95(9):1215–1218, 2005.

[82]Solomon, M., K. Guo, G. Sudlow, M. Berezin, W. Edwards, S. Achilefu, and W. Akers. Detection of enzyme activity in orthotopic murine breast cancer by fluorescence lifetime imaging using a fluorescence resonance energy transfer-based molecular probe. *J. Biomed. Opt.* 16(6):066019, 2011.

[83]Sonn, G., S. Jones, T. Tarin, C. Du, K. Mach, K. Jensen, and J. Liao. Optical biopsy of human bladder neoplasia

with in vivo confocal laser endomicroscopy. *J. Urol.* 182(4):1299–1305, 2009.

[84]Stuchinskaya, T., M. Moreno, M. J. Cook, D. R. Edwards, and D. A. Russell. Targeted photodynamic therapy of breast cancer cells using antibody–phthalocyanine–gold nanoparticle conjugates. *Photochem. Photobiol. Sci.* 10(5):822, 2011.

[85]Tan, J., M. Quinn, J. Pyman, P. Delaney, and W. McLaren. Detection of cervical intraepithelial neoplasia in vivo using confocal endomicroscopy. *BJOG* 116(12):1663–1670, 2009.

[86]Tauber, S., P. Schneede, B. Liedl, F. Liesmann, D. Zaak, and A. Hofstetter. Fluorescence cytology of the urinary bladder. *Urology* 61(5):1067–1071, 2003.

[87]Theodossiou, T., J. Hothersall, W. De Witte, A. Pantos, and P. Agostinis. The multifaceted photocytotoxic profile of hypericin. *Mol. Pharm.* 6(6):1775–1789, 2009.

[88]Thong, P. S. P., M. Olivo, W. W. L. Chin, R. Bhuvaneswari, K. Mancer, and K. C. Soo. Clinical application of fluorescence endoscopic imaging using hypericin for the diagnosis of human oral cavity lesions. *Br. J. Cancer* 101(9):1580–1584, 2009.

[89]Thong, P. S. P., M. Olivo, K. W. Kho, W. Zheng, K. Mancer, M. Harris, and K. C. Soo. Laser confocal endomicroscopy as a novel technique for fluorescence diagnostic imaging of the oral cavity. *J. Biomed. Opt.* 12(1):014007, 2007.

[90]Thong, P. S. P., M. Olivo, F. Lin, H. S. Seah, S. S. Tandjung, K. Qian, W. W. L. Chin, R. Bhuvaneswari, K. Mancer, and K. C. Soo. Detection and diagnosis of human oral cancer using hypericin fluorescence endoscopic imaging interfaced with embedded computing. *Proc. SPIE* 7380:73806U1-10, 2009.

[91]Thong, P., M. Olivo, M. Movania, S. Tandjung, H. Seah, F. Lin, K. Qian, and K. Soo. Hypericin fluorescence imaging of oral cancer: from endoscopy to real-time 3-dimensional endomicroscopy. *J. Med. Imaging Health Inform.* 1:1–5, 2011.

[92]Troutman, T., J. Barton, and M. Romanowski. Optical coherence tomography with plasmon resonant nanorods of gold. *Opt. Lett.* 32(11):1438–1440, 2007.

[93]Vandepitte, J., M. Roelants, C. Van, K. Hettinger, E. Lerut, P. Van, and W. de Witte. Biodistribution and photodynamic effects of polyvinylpyrrolidone-hypericin using multicellular spheroids composed of normal human urothelial and t24 transitional cell carcinoma cells. *J. Biomed. Opt.* 16(1):018001, 2011.

[94]Vasudevan, S., G. Chen, M. Andika, S. Agarwal, P. Chen, and M. Olivo. Dynamic quantitative photothermal monitoring of cell death of individual human red blood cells upon glucose depletion. *J. Biomed. Opt.* 15(5):057001, 2010.

[95]von Maltzahn, G., A. Centrone, J. H. Park, R. Ramanathan, M. J. Sailor, T. A. Hatton, and S. N. Bhatia. Sers-coded gold nanorods as a multifunctional platform for densely multiplexed near-infrared imaging and photothermal heating. *Adv. Mater.* 21(31):3175–3180, 2009.

[96]von Maltzahn, G., J. H. Park, A. Agrawal, N. K. Bandaru, S. K. Das, M. J. Sailor, and S. N. Bhatia. Computationally guided photothermal tumor therapy using long-circulating gold nanorod antennas. *Cancer Res.* 69(9):3892–3900, 2009.

[97]Wynn, J., and T. Cotton. Spectroscopic properties of hypericin in solution and at surfaces. *J. Phys. Chem.* 99(12):4317, 1995.

[98]Xiaojing, M., S. Winston, F. Hanhua, Y. Aibin, W. S. C. Kelvin, F. Chit-Yaw, and O. Malini. Mems micromirror integrated endoscopic probe for optical coherence tomography bioimaging. *EMBO J.* 21(22):5955, 2002.

[99]Xie, H., H. Liu, P. Svenmarker, J. Axelsson, C. Xu, S. Gräfe, J. Lundeman, H. Cheng, S. Svanberg, N. Bendsoe, P. Andersen, K. Svanberg, and S. Andersson-Engels. Drug quantification in turbid media by fluorescence imaging combined with light-absorption correction using white monte carlo simulations. *J. Biomed. Opt.* 16(6):066002, 2011.

[100]Yamazaki, T., N. Ohta, I. Yamazaki, and P. Song. Excited-state properties of hypericin: electronic spectra and fluorescence decay kinetics. *J. Phys. Chem.* 97(30):7870, 1993.

[101]Yang, Y., F. Li, L. Gao, Z. Wang, M. Thrall, S. Shen, K. Wong, and S. Wong. Differential diagnosis of breast cancer using quantitative, label-free and molecular vibrational imaging. *Biomed. Opt. Express* 2(8):2160, 2011.

[102]Yang, V., J. Yeow, L. Lilge, J. Kost, T. Mang, and B. Wilson. Noncontact point spectroscopy guided by two-channel fluorescence imaging in a hamster cheek pouch model. *SPIE Proc.* 3595:2, 1999.

[103]Yao, J., K. Maslov, Y. Zhang, Y. Xia, and L. Wang. Label-free oxygen-metabolic photoacoustic microscopy in vivo. *J. Biomed. Opt.* 16(7):076003, 2011.

[104]Yermak, P., N. Gamaleia, A. Shalamay, T. Saienko, and V. Kholin. Hyperflav—perspective photosensitizer for PDT: cell studies. *Exp. Oncol.* 32(4):233–236, 2010.

[105]Yong, K. T., I. Roy, M. T. Swihart, and P. N. Prasad. Multifunctional nanoparticles as biocompatible targeted probes for human cancer diagnosis and therapy. *J. Mater. Chem.* 19(27):4655, 2009.

[106]Zaak, D., D. Frimberger, H. Stepp, S. Wagner, R. Baumgartner, P. Schneede, and M. Siebels. Quantification of 5-aminolevulinic acid induced fluorescence improves the specificity of bladder cancer detection. *J. Urol.* 166(5):1665–1669, 2001.

[107]Zaak, D., M. Kriegmair, H. Stepp, R. Baumgartner, R. Oberneder, P. Schneede, S. Corvin, D. Frimberger, and R. Knuchel. Endoscopic detection of transitional cell carcinoma with 5-aminolevulinic acid: results of 1012 fluorescence endoscopies. *Urology* 57(4):690–694, 2001.

[108]Zaak, D., H. Stepp, R. Baumgartner, P. Schneede, R. Waidelich, D. Frimberger, A. Hartmann, R. Künchel, A. Hofstetter, and A. Hohla. Ultraviolet-excited (308 nm) autofluorescence for bladder cancer detection. *Urology* 60(6):1029–1033, 2002.

[109]Zaak, D., W. Wieland, C. Stief, and M. Burger. Routine use of photodynamic diagnosis of bladder cancer: practical and economic issues. *Eur. Urol. Suppl.* 7(7):536–541, 2008.

[110]Zara, J., S. Yazdanfar, K. Rao, J. Izatt, and S. Smith. Electrostatic micromachine scanning mirror for optical coherence tomography. *Opt. Lett.* 28(8):628–630, 2003.

[111]Zeisserlabouebe, M., N. Lange, R. Gurny, and F. Delie. Hypericin-loaded nanoparticles for the photodynamic treatment of ovarian cancer. *Int. J. Pharm.* 326(1–2):174–181, 2006.

[112]Zheng, W., K. C. Soo, R. Sivanandan, and M. Olivo. Detection of squamous cell carcinomas and pre-cancerous lesions in the oral cavity by quantification of 5-aminolevulinic acid induced fluorescence endoscopic images. *Lasers Surg. Med.* 31(3):151–157, 2002.

[113]Zhu, J., K. T. Yong, I. Roy, R. Hu, H. Ding, L. Zhao, M. T. Swihart, G. S. He, Y. Cui, and P. N. Prasad. Additive controlled synthesis of gold nanorods (GNRS) for two-photon luminescence imaging of cancer cells. *Nanotechnology* 21(28):285106, 2010.